Angular distribution of Ga^+ ions desorbed by 3-keV ion bombardment of GaAs(110)

Rik Blumenthal* and Nicholas Winograd
The Pennsylvania State University, 152 Davey Laboratory, University Park, Pennsylvania 16802
(Received 19 April 1990)

Angular distributions of Ga^+ ions desorbed from GaAs(110) surfaces by 3-keV Ar^+-ion bombardment under low-dose conditions have been determined. The distributions exhibit a high degree of anisotropy along the $\langle \bar{1}00 \rangle$ crystallographic direction with smaller peaks observed in several other specific directions. Using simple geometric analyses and with microscopic insight extracted from results of molecular-dynamics computer simulations on Si(110), we have been able to identify the scattering mechanisms that give rise to these peaks. The most dominant feature is found to arise from a specific collision sequence wherein a surface atom is ejected by direct collisions with a second-layer atom along the bond direction. This mechanism is interesting in that it contrasts with the channeling and blocking mechanisms previously reported for fcc metals. The position of other peaks in the angular distributions have been determined with use of simple geometrical arguments. We also examine the expected effect of the known GaAs(110) surface reconstruction on the observed patterns. These results should prove useful for testing molecular-dynamics calculations on ion-bombarded GaAs targets and may ultimately lead to a new approach to examining the surface structure of these types of complex materials.

I. INTRODUCTION

In recent years, there has been significant progress in understanding the interaction of keV particles with solids on an atomic scale. Experimental measurements of the energy and angular distribution of desorbed particles have been made on a variety of clean and adsorbate-covered single-crystal surfaces.[1-6] Detection is now possible for both secondary ions[1-5] and neutral atoms[6] desorbed by low-dose ion bombardment where surface damage is minimized. An atomic-level understanding of these interactions has been obtained through comparisons of experimental distributions and molecular-dynamics computer simulations. These calculations yield nuclear motion of the atoms in the solid, using many-body potential functions to describe the force fields.[7]

For ion-induced desorption form Rh(111), an fcc metal, excellent agreement between the calculated and experimental energy and angular distributions of ejected Rh atoms has been achieved using the embedded-atom method (EAM) in dynamical simulations.[8] An important mechanistic feature which has emerged from these and related simulations is that the ejected particles are strongly channeled and blocked by other surface atoms. These effects systematically influence the angular distributions and allow for the determination of the structure of clean and adsorbate-covered single-crystal surfaces.[1-6]

There have been several recent molecular-dynamics simulations performed to examine the dynamics of ion-bombarded Si crystals.[9-11] A basic understanding of the response of these materials to bombardment is important in explaining the characteristics of microelectronic devices constructed using ion implantation or reactive ion etching. These covalently bonded materials have been very difficult to model theoretically because of the directional nature of the bonding and also because of the dramatic reconstructions these surfaces often undergo. The latest results,[9] utilizing an empirically derived many-body potential, suggest that the basic mechanisms of ejection of Si atoms are quite different than the channeling and blocking mechanisms that dominate angular distributions of ion-bombarded metal surfaces. The important difference is that for Si there are large open channels where atoms can move unimpeded. In addition to the channeling and blocking mechanisms, evidence has been found for atom-atom collisions that lead to desorption along the nearest-neighbor bond directions. These simulations qualitatively support early experimental angular distributions for Si^+ desorbed from ion bombarded Si(100).[12]

In this paper the first angular distributions of ions ejected from clean GaAs(110) under low-dose conditions are presented. At this point, accurate many-body potential have not yet been developed to describe the response of GaAs to energetic particle bombardment. From a detailed analysis of the angular distributions of Ga^+ ions, however, we show that the primary mechanism of ion-induced desorption differs substantially from that observed for fcc metals. Specifically, we find that the dominant ejection mechanism involves a specific collision sequence wherein a surface atom is ejected by direct collision with a second layer atom along the bond direction. These results support the qualitative descriptions of the ion-solid interaction event obtained from molecular dynamics simulations on Si(110) and provide an important base of data for future computer simulations of the ion bombardment of GaAs. Moreover, the sensitivity of our data to the nature of the surface reconstruction suggest that these angular distributions may provide important surface structural information from rather complex systems.

II. EXPERIMENT

All measurements were performed using an angle-resolved secondary-ion mass spectroscopy (SIMS) apparatus described elsewhere.[13] Briefly, the ultrahigh-vacuum (UHV) chamber was equipped with low energy electron diffraction (LEED), Auger electron spectroscopy (AES), a differentially pumped Leybold-Heraeus ion source, and an Extrel C50 quadrupole mass spectrometer (QMS). The polar angle of detection could be altered independently by rotation of the differentially pumped QMS mounting flange. The QMS was equipped with an input einzel lens with an acceptance aperture of 1.8 mm positioned 3.7 cm from the center of the experimental chamber and a 90° electrostatic sector for energy selection. This results in a total polar angular acceptance of ±3° and a typical energy acceptance of 20.0±0.2 eV. The crystal manipulator allowed independent translation along three Cartesian axes and independent rotation around two perpendicular axes parallel and perpendicular to the sample surface.

There are three important angle designations of relevance to these experiments. The azimuthal angle is defined in the plane of the crystal surface, and is referenced to the ⟨100⟩ direction on the surface as noted in Fig. 1. The incidence angle is defined as the angle between the surface normal and the ion source. The polar detection angle or ejection angle is the angle between the detector aperture and the surface normal. The three angles can be determined to a precision ±1° and set to an accuracy of ±0.1°. The total angular distribution is collected as a series of azimuthal angle scans at a fixed polar angle. Each scan is obtained by rotation of the sample in one-degree steps over three full revolutions. The angle positions are set by computer controlled stepping motor. For the data reported here, intensities of the various azimuthal scans, taken on different days, were normalized to a scan of the polar detection angle. Azimuthal scans were not corrected for the increase in azimuthal acceptance as the polar detection angle was decreased. This effect results in azimuthal acceptances of 3.3° and 1.5°, at polar angles of 25° and 70°, respectively.

Undoped, semi-insulating GaAs(110) wafers were obtained from M/A Com Laser Diodes. The wafers were cleaved into pieces and degreased in trichloroethane, acetone, ethanol, and methanol before etching in a 1:1:5 solution of peroxide:water:sulfuric acid. The (110) face was found to be oriented within ±0.5° by Laue x-ray diffraction. Each sample was attached with In to a Mo block which was mounted onto the manipulator. Sample heating was provided by an electron bombardment source located behind the Mo block.

All surfaces were prepared by cycles of ion bombardment and annealing to 585 °C for 2 min. This procedure provided a clean and ordered surface as determined by LEED, AES, and SIMS. The total ion dose during experiments was maintained at static levels by limiting the exposure time to less than one-tenth of the time required to desorb one monolayer of GaAs. This was accomplished by focusing a 2-nA beam into a 1-mm spot located 3 mm from the rotation axis of the crystal. During an azimuthal scan the entire wafer was slowly rotated through three full 360° revolutions over a time of about 45 min. To ensure that the crystal edges were playing no role in the observed features, experiments were carried out on two crystals of vastly different shapes. No distinguishable differences in the patterns could be discerned. We were only successful at detecting the Ga^+ ions under static conditions. The incident ion flux had to be increased to unacceptable levels to achieve any discernible As^- signal.

Ion collection over three full rotations served several purposes. First, the influence of beam damage could be minimized and carefully monitored since a virgin area of the crystal was constantly being exposed to the beam. Second, the data could be conveniently averaged. Final-

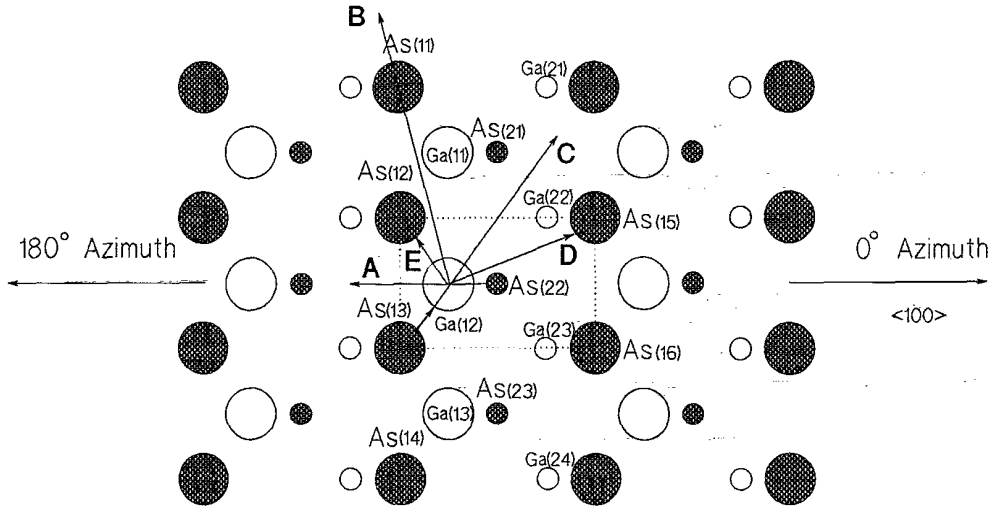

FIG. 1. The structure of the unreconstructed GaAs(110) surface. The open and hatched circles represent Ga and As atoms, while the larger and smaller circles represent atoms in the first and second layers, respectively. The arrows indicate the various channeling and blocking directions suggested by this structure.

ly, each scan could be set to begin at the same azimuth at which the previous scan had ended. This feature provided a consistent reference of the azimuths between scans of different polar angles even for dramatically different patterns.

III. RESULTS AND DISCUSSION

The angular distribution of Ga^+ ions ejected from GaAs(110) is shown in Fig. 2. As seen in the figure the distribution could be obtained at each azimuthal angle between 0° and 360° for a series of polar angles between 25° and 70°. These data are clearly characterized by a high degree of symmetry and anisotropy. The striking feature of our results is the single, intense Ga^+ ion peak observed at a polar angle of 35° and at an azimuthal angle of 180°. Other features are positioned with nearly mirror plane symmetry about this major peak. At higher polar angles, other maxima and minima are observed at various azimuthal angles. It is our goal to associate these anisotropies with the known surface structure of GaAs(110) and hence to determine the mechanistic details of the ion-solid interaction.

The atomic structure of the bulk terminated GaAs(110) surface is shown in Fig. 1. The surface chain appears as a vertical zigzag row of alternating As and Ga atoms. The second-layer atoms, as denoted by the smaller circles, are positioned with a similar geometry. It has been known from LEED measurements[14] that the surface reconstructs extensively by a bond length conserving surface chain rotation of ~29°. More specifically, reconstruction involves the movement of surface Ga atoms into the crystal surface, and away from the second layer As atoms, while the movement of the surface As is out of the surface, and toward the second layer Ga atoms. This structure has been verified independently by a variety of techniques including angle-resolved photoemisson,[15,16] isochromat spectroscopy,[17,18] medium energy ion scattering,[19] and shadow cone enhanced SIMS.[20]

The most prominent features of the angular distribution shown in Fig. 2 can be explained in a rather straightforward fashion if it is assumed that the most favorable Ga^+ ion ejection mechanism involves direct atom-atom collisions along the bond directions. For example, the pronounced peak in the Ga^+ ion distribution at $\theta=35°$ and $\phi=180°$ would arise from collisions between the second-layer As atom, As(22), and the surface Ga atom, Ga(12), along the direction of their common bond. The mechanism is illustrated with arrow A shown in Fig. 1. Note that no such mechanism is possible along $\phi=0°$, accounting for a lack of significant signal along this azimuth. As we shall see, several other peaks in the distribution may also be explained in a straightforward fashion.

To more quantitatively interpret the origin of the features apparent in Fig. 2, it is really necessary to perform computer simulations of the ion-impact event. Unfortunately, classical dynamics computer simulations are not yet available for GaAs crystals to help us with this problem. There have been recent attempts, however, to determine the angular distributions of Si atoms ejected from the Si(110) surface.[9,10] It is feasible to utilize these calculations in making assignments of at least the most prominent features in the angular distributions measured

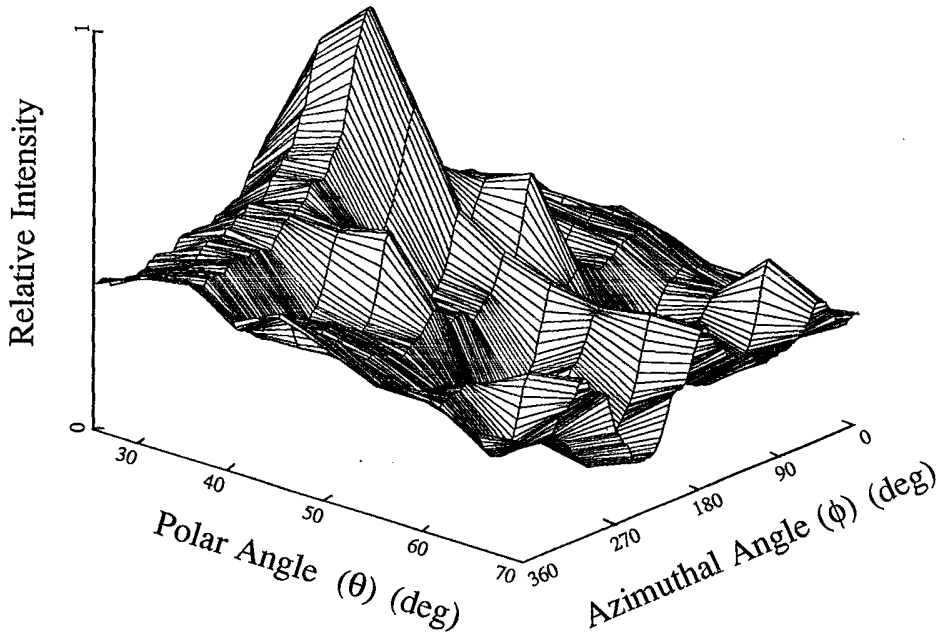

FIG. 2. The ion-induced angular distribution of Ga^+ ions desorbed by 3-keV normal incident Ar^+ ion bombardment of GaAs(110). The polar angle refers to the angle of detection from the surface normal. The azimuthal angle is referenced to the ⟨100⟩ direction on the crystal surface. The energy of the ions detected was 20.0±0.2 eV, and the distribution is shown for a fixed total angle of acceptance.

from GaAs. The bulk crystal structure of the two materials is, of course, closely related. Moreover, previous calculations of these distributions have shown that the response of a solid to keV ion bombardment is influenced more strongly by structure than by chemical bonding forces.[1–4,7] The same basic azimuthal angle distribution is found for Cu(111)[1] and for Rh(111),[6] for example, even though there may be small differences in the relative intensities of the maxima and in the values of the angles associated with the peaks in the polar angle distributions. The calculated distribution of Si atoms ejected from an artificial bulk-terminated Si(110) surface with kinetic energies between 10 and 30 eV is shown in Fig. 3. This plot was obtained from the calculated distribution of Si atoms by selecting only those ejected atoms that would be Ga atoms in the GaAs(110) crystal.

This distribution yields surprisingly good agreement with the experimental distribution of Fig. 2. A single, prominent peak is found at $\theta=38°$ and $\phi=180°$. Even the smaller features near $\phi=90°$ and 270° at $\theta>50°$ also seem to have a tentative correspondence with the experimental data. The computer simulations clearly show that a significant number of ejected atoms that make up the peak along $\phi=180°$ arise from ejection of a surface Ga atom by the direct collision of a second-layer As atom along the direction of their common bond.[9]

This type of mechanism is quite different than that discussed for the ejection of metal atoms from single crystal metal surfaces. For metals, the most important origin for the angular anisotropies arises from channeling and blocking of the ejecting first-layer atoms by other surface atoms. Atom-atom collisions contribute only a small intensity to the distributions. For example, the Rh(111) surface with two different threefold symmetric open azimuthal directions only displays a 20% enhancement in the neutral atom ejection yield along the "hcp" direction.[18] The classical dynamics simulations reveal that this effect is due to a specific collision sequence of second-layer atoms colliding with surface-layer atoms and ejecting them along their bond directions. Thus, there is precedence for the contribution of atom-atom collisions to the ejection process, although it appears to be much more important in covalent crystals such as Si and GaAs.

It is instructive to quantitatively compare the experimental and calculated values of the polar angle of maximum intensity. We believe it is reasonable to make this comparison even though we have chosen to detect Ga^+ ions in the SIMS mode rather than neutral Ga atoms. Preliminary experimental polar angle distributions along $\phi=180°$ for the neutral distribution as obtained with a multiphoton resonance ionization detection scheme,[21] and for Ga^+ ions, is shown in Fig. 4. Both distributions peak at the same polar angle and exhibit the same general features. Apparently, in this kinetic energy regime, there is only a minimal effect of angle-dependent ionization probabilities and of the image potential, in contrast with what has been observed from metal surfaces.

As noted above, the Si yield along $\phi=180°$ maximizes at a polar angle of 38°. If the desorption of Si occurred directly along the bond direction, it would be expected to occur at $\theta=35°$, obviously very close to the calculated value. Both of these values are obtained for a bulk-terminated Si(110) surface. For our experiments on

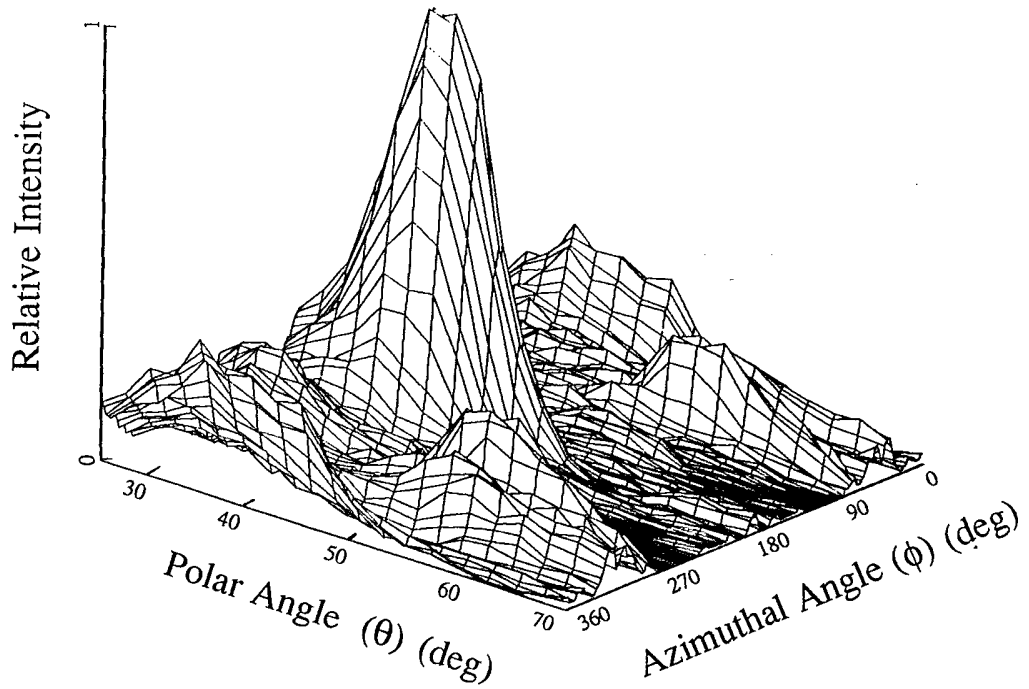

FIG. 3. The calculated angular distribution of secondary Si atoms, with kinetic energies between 10 and 30 eV, desorbed from Si(110) by 1-keV Ar^+ ion bombardment. The angular distribution is shown with reduced symmetry to allow for the direct comparison with the experimental Ga^+ ions distributions for Ga^+ ions desorbed from GaAs(110).

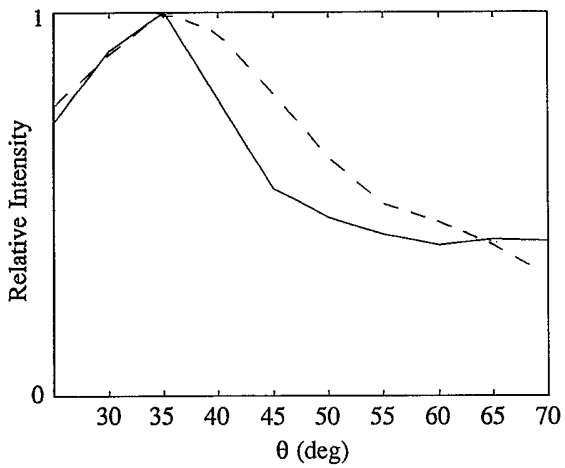

FIG. 4. The polar distribution of 20-eV Ga^+ ions (solid line) and Ga atoms, with kinetic energies between 20 and 50 eV (broken line) desorbed from GaAs(110).

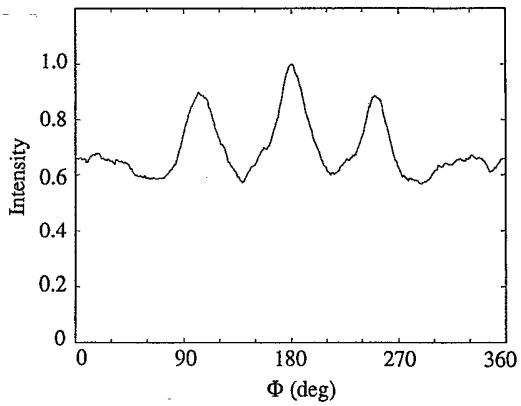

FIG. 5. The relative intensity of 20-eV Ga^+ ions desorbed from GaAs(110) as a function of azimuthal angle at a polar angle of 45° from the surface normal.

GaAs(110), the peak in the polar angle along $\phi=180°$ is also observed at $\theta=35°$. For this system, however, the topmost Ga atom moves downward by 0.50 Å and the topmost As atom moves outward by 0.15 Å. This chain rotation increases the As(22)—Ga(22) bond angle to 44° with respect to the surface normal, a value nearly 10° larger than that found experimentally. The difference presumably arises by distortions created by As(12) and As(13). After the reconstruction they are in a position to focus ejecting Ga atoms closer to the surface normal. In future experiments and simulations, it will be interesting to see if such distortions are, in fact, quantitatively calculable. Such measurements would provide a straightforward procedure for determining a number of rather subtle surface structures.

Finally, the Si computer simulations suggest that a significant portion of the intensity in this major peak may consist of Ga^+ ions ejected from the second layer which are focused into this same angular region.[9] It is not possible for us to experimentally distinguish between first and second-layer Ga^+ ions. At this point, then, we cannot confirm this intriguing prediction of the computer simulations.

The next set of structurally significant features apparent from the distributions shown in Fig. 2 occur at an exit angle of $\theta=45°$. The azimuthal angle distributions are shown in Fig. 5. For this case, an additional pair of peaks is observed at $\phi=102°$ and $\phi=252°$. This structure could potentially originate from a large group of channeling mechanisms. The computer simulations on Si, however, show that these features arise mainly from the ejection of Ga(12) through the channel created by As(12) and Ga(11). Assuming that the particles move midway between As(12) and Ga(11), this direction is expected to be found at 76° on either side of the $\phi=180°$ azimuth at $\phi=104°$ and at $\phi=256°$. These predictions are in close agreement with the peak positions shown in Fig. 5. The channeling direction is denoted by arrow B in Fig. 1 and the relevant angles are summarized in Table I. We suspect that this mechanism is made somewhat more favorable by the fact that As(12) is moved up and out of the surface plane of the reconstructed surface, hence opening the channel slightly. The calculated distribution again shows a component of second-layer atoms in this peak, and thereby justifies consideration of their possible contribution to the intensity of these peaks. However, no specific mechanism leading to the focusing of second-layer atoms into these peaks can easily be found.[9] The fact that the experimental azimuthal spectra do not exhibit perfect experimental mirror plane symmetry about 180° azimuth is presumably a manifestation of unknown imperfections in the GaAs(110) crystal surface. These small asymmetries are only apparent at polar angles greater than 40°, angles where these effects might be expected to most strongly influence the results.

A similar azimuthal angle distribution is obtained at $\theta=65°$ as shown in Fig. 6. In this case, however, a small peak at $\phi=0°$ is observed, presumably due to channeling of Ga(12) along this direction after it has received momentum from lattice atoms moving in random directions. Moreover the computer simulations show that by As(15) and As(16) the channeling mechanism *B* is no longer possible. Instead, Ga(12) is ejected by As(13) after the latter has been driven down into the crystal. For metal surfaces, this has been referred to as the "up-down" mechanism, and it generally propagates through a close-packed row. The GaAs lattice is much more open, so Ga(12) may escape directly along the As(13)—Ga(12) bond axis. This mechanism is denoted by arrow *C* in Fig. 1 and should occur at $\phi=55°$ and $\phi=305°$ as summarized in Table I. Note that the experimental values of $\phi=52°$ and $\phi=306°$ are in close agreement with this assignment.

Two sets of minima are apparent in Fig. 6. The first set is seen at $\phi=26°$ and $\phi=334°$ and is due to blocking of Ga(12) by As(15). The second set is seen at $\phi=116°$ and $\phi=237°$ and is due to blocking of Ga(12) by As(12). The mechanisms are denoted by arrows *D* and *E*, respectively, and are also summarized in Table I.

In general, there is close agreement between the positions of the peaks and valleys of the azimuthal distributions as expected from simple trigonometric arguments

TABLE I. Comparison of calculated and measured channeling and blocking features on GaAs(110).

Mechanism[a]	Calculated[b]	Fig.	Measured	Type	Observed as
A	0°	6	0°	Channeling	Maximum
	180°	2, 5, 6	180°		
B	104°	5	102°	Channeling	Maximum
	256°	5	252°		
C	55°	6	52°	Up-down	Maximum
	305°	6	306°		
D	25°	6	26°	Blocking	Minimum
	335°	6	334°		
E	123°	6	116°	Blocking	Minimum
	235°	6	237°		

[a]See Fig. 1 for the definition of these mechanisms.
[b]Azimuthal angle ϕ calculated from simple trigonometry as indicated in Fig. 1 and in the text.

without including the influence of the GaAs(110) surface reconstruction on these distributions. The net effect of the reconstruction is to shorten the lateral spacing of the surface Ga and As atoms, thereby increasing the expected angular spacing of the blocking features. The chain rotation of 29° results in a change of the predicted positions of the appropriate maxima and minima by only about 3°. This small difference is really beyond the error limits of our simple models. Moreover, at this stage it is not completely clear how to assign a specific angle to a blocking feature. In the absence of any model of the shape of these features, the blocking angle was arbitrarily determined at the intensity minima. Other scenarios for picking this angle are equally likely. For instance, along the 180° azimuth it can be seen that inner edges of the As atoms are quite close to the ejecting Ga atoms. These ejecting atoms are likely to interact strongly with both surface As atoms. This three-body interaction would result in intensity distributions whose edges near the 180° azimuth are displaced away from the azimuth, resulting in error. We believe that both the surface reconstruction and distortions due to the blocking atoms are playing a role in the quantitative discrepancy observed along the 180° azimuth, but the qualitative agreement certainly supports our assignments.

The anisotropy observed at $\theta=45°$ is extremely sensitive to ion damage of the surface. The ion yield at a 45° degree angle of detection under two different ion fluxes is shown in Fig. 7. The solid line shows the ion yield with a beam current of 1.6 nA while the dotted line is the ion yield of the next consecutive scan where the beam current has been increased to 5.5 nA. These data demonstrate not only the reproducibility of the three peaks observed along the 180° azimuth, but also the decay of signal as a function of ion dose. It should be noted that the curve at lower ion fluence shows no significant decrease in peak intensity over the three revolutions, while the high fluence curves shows a continuous decrease in signal intensity. The patterns of desorption from surfaces having sustained a significant amount of ion-induced damage have also been determined, and differ drastically from those of ordered surfaces. For instance, the pattern at 45° angle of detection from a heavily damaged surface, seen in Fig. 8, shows only one broad peak at the 180° azimuth

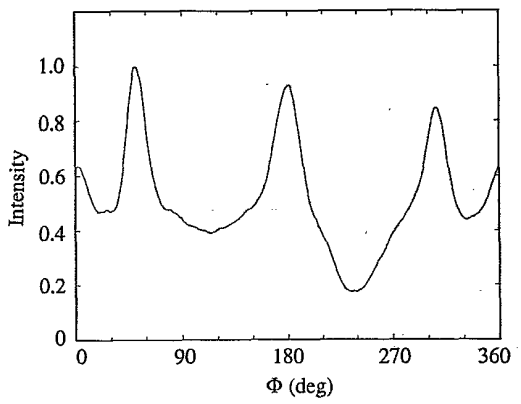

FIG. 6. The relative intensity of 20-eV Ga^+ ions desorbed from GaAs(110) as a function of azimuthal angle at a polar angle of 65°.

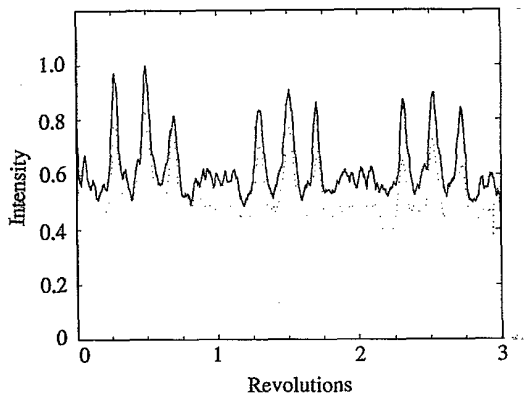

FIG. 7. The relative intensity of 20-eV Ga^+ ions desorbed from GaAs(110) obtained during three complete revolutions of the crystal at a polar angle of 45° with ion beam currents of 1.6 nA (solid line) and 5.5 nA (broken line). he intensity of the distribution at 1.6 nA has been multiplied by 3.6 to provide for the direct comparison of the two curves.

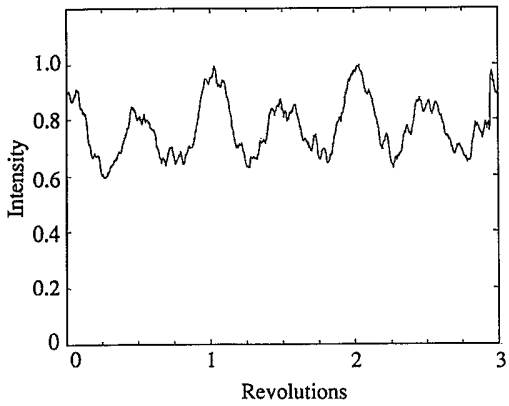

FIG. 8. The relative intensity of 20-eV Ga^+ ions desorbed from an ion beam amorphized GaAs(110) surface obtained during three complete revolutions of the crystal.

in contrast with the three sharp peaks observed from an ordered surface.

The sensitivity of the characteristic three-peak pattern of the azimuthal distribution at a polar angle of 45° was exploited as an *in situ* monitor of ion-induced damage. After each cycle of ion bombardment and annealing, an azimuthal scan at a polar angle of 45° was collected. The resulting anisotropy was used as the criterion for continuing the experiment by changing the polar angle of detection and collecting more azimuthal spectra or terminating the experiment due to poor surface order. Also, at the end of each series of experiments a scan of the azimuthal distribution at a polar angle of 45° was acquired to judge the cumulative effect of the total ion dose.

A few final aspects of the angular distributions deserve further discussion. First, in each azimuthal spectra there exists a significant baseline signal. This signal is believed to be due to disordered areas of the surface generated by either the ion bombardment or annealing. In Figs. 2 and 6, the intensity minima around the 180° azimuth do not dip to zero signal levels and are, in fact, unequal in intensity. The failure to drop to zero intensity is also attributed to disordered areas of the surface, while the unequal intensities may arise from the presence of regions of the surface with an overlayer of metallic Ga. We believe that this overlayer exists as a "raft" similar to that formed by Al (Ref. 22) and is always present after ion bombardment or heating.

IV. CONCLUSION

We have presented, for the first time, the angular distribution of Ga^+ ions desorbed from the GaAs(110) surface by 3-keV Ar^+-ion bombardment. From a simple geometric analysis of the ion-induced desorption pattern, we find that the mechanism of ion ejection from this surface is drastically different from the blocking and channeling observed previously on metal surfaces.[1–6] Specifically, the ejection of Ga^+ ions into a single peak, at 35° from the surface normal and along the 180° azimuth, dominates the distribution and is attributed to a direct ejection mechanism in which a second layer As atom collides with a surface Ga atom, causing it to desorb along their common bond direction. Although the geometric analysis provides an excellent qualitative explanation of the observed desorption pattern, some quantitative disagreements remain between the geometric analysis and the observed distribution. The development of a suitable potential for use in full dynamics calculations of the ion bombardment of GaAs should allow for the resolution of the uncertainties that exist in the analysis and provide for the accurate determination of surface structures from the angular distributions of ion-induced secondary ions.

We believe that this work has demonstrated that the angular distribution of secondary ions contains a wide variety of information about both the surface structure and the mechanisms of momentum transfer which result in ion desorption. The results not only serve to increase our understanding of the ion-solid interaction itself, but also suggest that angle-resolved SIMS may become a unique tool for the characterization of a wide variety of complex structures associated with semiconductor surfaces. Of particular interest is the study of molecular beam epitaxially grown GaAs(100) which displays a number of surface reconstructions. These surfaces can be prepared in our growth chamber and transferred under UHV conditions to our analysis chamber.

ACKNOWLEDGMENTS

The authors are grateful to Barbara Garrison and Roger Smith for supplying the results of their Si(110) calculations. We also appreciate the encouragement of Ehud Furman, Susan Donner, Raj Trehan, Brad Weaver, and especially Kevin Caffey. We thank the Office of Naval Research, the National Science Foundation, the donors of the Petroleum Research Fund administered by the American Chemical Society and the IBM Corporation for generous financial support.

*Present address: Department of Chemistry, California Institute of Technology, Pasadena, CA 91125.

[1]S. P. Holland, B. J. Garrison, and N. Winograd, Phys. Rev. Lett. **43**, 220 (1979).

[2]S. P. Holland, B. J. Garrison, and N. Winograd, Phys. Rev. Lett. **44**, 756 (1980).

[3]R. A. Gibbs, S. P. Holland, K. E. Foley, B. J. Garrison, and N. Winograd, J. Chem. Phys. **76**, 684 (1982).

[4]D. W. Moon, R. J. Bleiler, and N. Winograd, J. Chem. Phys. **85**, 1097 (1986).

[5]N. Winograd, *Desorption Mass Spectrometry* (The American Chemical Society, Washington, D.C., 1985), pp. 83–96.

[6]N. Winograd, P. H. Kobrin, G. A. Schick, J. Singh, J. P. Baxter, and B. J. Garrison, Surf. Sci. **176**, L817 (1986).

[7]D. E. Harrison, Jr., Crit. Rev. Sol. St. Mat. Sci. **14**, s1 (1988).

[8]B. J. Garrison, N. Winograd, D. M. Deaven, C. T. Reimann,

D. Y. Lo, T. A. Tombrello, D. E. Harrison, Jr., and M. H. Shapiro, Phys. Rev. B **37**, 7197 (1988).
[9]R. Smith, D. E. Harrison, Jr., and B. J. Garrison, Phys. Rev. B **40**, 93 (1989).
[10]R. A. Stansfield, K. Broomfield, and D. Clary, Phys. Rev. B **39**, 7680 (1989).
[11]R. Smith, D. E. Harrison, Jr., and B. J. Garrison, *Secondary Ion Mass Spectrometry (SIMS VII)* (Wiley and Sons, New York, 1989).
[12]R. J. MacDonald, Phys. Lett. **29A**, 256 (1969); Radiat. Eff. **3**, 131 (1970).
[13]R. Blumenthal, E. Furman, B. Weaver, K. Caffey, S. K. Donner, J. Herman, Raj Trehan, and N. Winograd (unpublished).
[14]A. R. Lubinsky, C. B. Duke, B. W. Lee, and P. Mark, Phys. Rev. Lett. **36**, 1058 (1976).
[15]A. Huijer, J. VanLaar, and T. L. van Rooy, Phys. Lett. **65A**, 335 (1978).
[16]J. A. Knapp and G. J. Lapeyre, J. Vac. Sci. Technol. **13**, 757 (1976).
[17]V. Dose, H.-J. Gossmann, and D. Straub, Phys. Rev. Lett. **47**, 608 (1981).
[18]V. Dose, H.-J. Gossmann, and D. Straub, Surf. Sci. **117**, 387 (1982).
[19]L. Smit, T. E. Derry, and J. F. van der Veen, Surf. Sci. **150**, 245 (1985).
[20]R. Blumenthal, S. K. Donner, J. L. Herman, R. Trehan, K. P. Caffey, E. Furman, and N. Winograd, J. Vac. Sci. Technol. **B6**, 1444 (1988).
[21]K. N. Walzl, R. Trehan, C. T. Reimann, M. El-Maazawi and N. Winograd (unpublished results).
[22]A. Zunger, Phys. Rev. B **24**, 4372 (1981).